Atmos. Chem. Phys. Discuss., 12, 4243–4278, 2012
www.atmos-chem-phys-discuss.net/12/4243/2012/
doi:10.5194/acpd-12-4243-2012

Atmospheric Chemistry and Physics Discussions

Determinants and predictability of global wildfire emissions

W. Knorr[1], **V. Lehsten**[1], **and A. Arneth**[2,1]

[1]Physical Geography and Ecosystem Analysis, Lund University, Sölvegatan 12, 22362 Lund, Sweden
[2]KIT/IMK-IFU, Kreuzeckbahnstr. 19, 82467 Garmisch-Partenkirchen, Germany

Received: 2 December 2011 – Accepted: 24 January 2012 – Published: 6 February 2012

Correspondence to: W. Knorr (wolfgang.knorr@gmail.com)

Published by Copernicus Publications on behalf of the European Geosciences Union.

Abstract

Biomass burning is one of the largest sources of atmospheric trace gases and aerosols globally. These emissions have a major impact on the radiative balance of the atmosphere and on air quality, and are thus of significant scientific and societal interest. Several datasets have been developed that quantify those emissions on a global grid and offered to the atmospheric modelling community. However, no study has yet attempted to systematically quantify the dependence of the inferred pyrogenic emissions on underlying assumptions and input data. Such a sensitivity study is needed for understanding how well we can currently model those emissions and what the factors are that contribute to uncertainties in those emissions estimates.

Here, we combine various satellite-derived burned area products, a terrestrial ecosystem model to simulate fuel loads and the effect of fire on ecosystem dynamics, a model of fuel combustion, and various emission models that relate combusted biomass to the emission of various trace gases and aerosols. We vary one key parameter of a simple fuel combustion model, the emission model, and the burned area product and assess its impact on the computed emissions fields and their uncertainties. We find that choice of burned area data set has by far the largest impact on interannual variability of simulated emissions. For total global emissions, burned area and combustion completeness have the largest impact on emissions for most species.

We conclude that reliable information on burned area is key for accurately modelling spatial and interannual variations of wildfire emissions, but uncertainties about the combustion process have a similar impact on the magnitude of global emission estimates. The results are important for chemical transport modelling studies, and for simulations of biomass burning impacts on the atmosphere under future climate change scenarios.

ACPD

12, 4243–4278, 2012

1 Introduction

Wildland fires have an important impact on the atmospheric load of trace gases and aerosols, on air pollution, and climate (Seiler and Crutzen, 1980; Langmann et al., 2009). Fire has also been recognized as an important agent in the workings of the Earth system, because it is an intrinsic feature of all terrestrial ecosystems outside Antartica and responds both to climate change and human intervention (Bowman et al., 2009; Arneth et al., 2010). In response, comprehensive datasets have been developed that characterize the extent of fires globally from satellite data (Grégoire et al., 2003; Simon et al., 2004; Roy et al., 2005; Mouillot and Field, 2005; Giglio et al., 2006, 2010; Tansey et al., 2008), as well as the chemical emissions from those fires (Schultz, 2002; Duncan et al., 2003; Hoelzemann et al., 2004; van der Werf et al., 2006, 2010; Schultz et al., 2008; Mieville et al., 2010). Those data sets can be used to study the effects of wildfires on air pollution and climate (Langmann et al., 2009), while others, that differentiate between types of biomass burning sources, are also useful for better characterizing the role of fires in the Earth system (e.g. van der Werf et al., 2010).

The next step forward will be to assess the possible future and (pre-instrumental) past impact of wildfires under the conditions of a changing climate. In contrast to the emission studies cited above, such an approach requires the use of a fully prognostic model of wildfire occurrence, which includes using a dynamic vegetation model for predicting the accumulation of fuels, to replace the use of satellite remote sensing data. However, while global dynamic vegetation models exist on a global scale that have been coupled to predictive fire models (Thonicke et al., 2001, 2010; Arora and Boer, 2005; Prentice et al., 2011), a comparison of simulated fractional area burned with those inferred from satellite data still shows large discrepancies (Thonicke et al., 2001, 2010; Prentice et al., 2011).

Prior to including fire in comprehensive Earth system models, it is therefore necessary to assess how reliably we are currently able to model the different steps necessary for computing chemical emissions from wildfires: characterization of area burned,

ACPD
12, 4243–4278, 2012

quantification of the amount of biomass combusted per area burned, and amount of chemical species emitted per unit amount of biomass combusted. Only if we better understand how sensitive simulated emissions are to uncertainties in each of these steps can we, for example, judge how well we need to reproduce burned area by prognostic models, or how accurately we need to simulate fuel loads and combustion factors.

The commonly used approach to compute pyrogenic emissions is to combine information on fire occurrence and extent with information on available fuel, combustion completeness (i.e. fraction of fuel combusted in a fire), and conversion rates of combusted fuel to the emitted amounts of various trace gases (Seiler and Crutzen, 1980). Relevant observations that cover the entire earth are available only from satellite remote sensing as counts of fire occurrence detected by radiant emissions from fires in the middle infrared (Matson and Dozier, 1981), or the detection of burn scars by analysing bidirectional surface reflectance (Govaerts et al., 2002; Roy et al., 2005).

Fuel load is more difficult to derive from remotely sensed information, because only the leaves of healthy vegetation can be reliably detected from space, while typical fuel provided by dead plant material cannot usually be distinguished from the soil background. Therefore, ecosystem models are often used to model fuel load (e.g. van der Werf et al., 2010), which depends not only on plant type distribution and climate, but also on the effect of the fires itself (Thonicke et al., 2010). Observations of the combustion process are even more difficult to obtain from the field, with the closest being observations of radiant energy from satellites, which can be used for estimating the total amount of energy generated by the fire (Wooster et al., 2005). Since this technique is still under development (Boschetti and Roy, 2009), the fraction of fuel combusted in a fire is usually an assumed or modelled value (Ito and Penner, 2004; Arora and Boer, 2005; Wiedinmyer et al., 2006; Thonicke et al., 2010).

The provision of emissions fields from biomass burning is already a useful and important step for the atmospheric modelling community, as it allows the assessment of how important pyrogenic emissions are for the total atmospheric trace gas or aerosol load, and their contribution to interannual variations and episodes (Langmann et al.,

ACPD
12, 4243–4278, 2012

2010). Modelled trace gas fields can be compared to those trace gases that are easy to observe, such as carbon monoxide, to evaluate chemical transport and emissions modelling together (Langenfelds et al., 2002). However, the variety of approaches to compute emissions leads one to suspect that the use of different observations and models will yield varying emissions fields, and any comparison between modelled and observed atmospheric trace gases or aerosol loads needs to take into account that a whole range of possible emissions fields exists, some of which may lead to better and some to worse agreement with atmospheric observations.

In this study, we pose the following questions: how well can we currently model chemical emissions from wildfires based on fire observations, and what is the consequence of these findings for our ability to simulate emissions under climate change?

2 Methods

We combine remotely sensed burned area with modelled fuel loads from the global dynamic vegetation model LPJ-GUESS (Smith et al., 2001). The flux of carbon from fire to the atmosphere computed by LPJ-GUESS is subsequently fed into a set of separate models to compute emissions of various trace gases. We explore the sensitivity of modelled chemical emissions to the different algorithms and parameterizations for emissions and fuel combustion, as well as remotely sensed burned area. We also propagate reported uncertainties in emission factors to the final results. Finally, we compare the sensitivity of modelled emissions to uncertainties in emission factors, to the choice of emission model, to the uncertainty range of one key fuel combustion parameter, and the choice of burned area input data. The purpose is to explore the general sensitivity of modelled wildfire emissions to various key inputs and parameterizations that may need further refinement or validation.

We deliberately choose a simple approach to fire modelling, instead of a fully prognostic fire model, in order to make the chain of factors entering the sensitivity study as transparent as possible. Instead of computing burned area and assessing how

ACPD
12, 4243–4278, 2012

different parameterisations of the burned area model affect the results, we use a variety of burned area products as input. The assumption here is that differences between global burned area products are similar in magnitude to the uncertainty in computed burned area of some prognostic modelling framework used to study fires under future or past climates.

2.1 Ecosystem and fuel combustion model

We use the Lund-Potsdam-Jena General Ecosystem Simulator (LPJ-GUESS) to compute the establishment, growth and mortality of potential natural vegetation, as well as plant and soil water status and plant litter accumulation on a global scale (Smith et al., 2001). Carbon, water and surface energy exchanges are computed on a daily time step, while establishment, growth, allocation, mortality by general disturbance and competition are simulated with a yearly time step. We use the global version of LPJ-GUESS with 13 plant functional types (PFTs), comprising nine tree and two grass PFTs (see Table 1). LPJ-GUESS is run in cohort mode, where groups of individuals of similar age and size, or "cohorts" are represented by a single individual. We run LPJ-GUESS with five patches per grid cell, and a stochastic general patch destroying disturbance with an average return interval of 100 yr.

As input data we use the gridded Climate Research Unit TS3.1 monthly observations of diurnal mean temperature, precipitation and percent of potential (full sunshine) insolation for the period 1901 to 2009 (Mitchell and Jones, 2005; Jones and Harris, 2011), following a spin-up procedure described by Sitch et al. (2003). Annual atmospheric CO_2 concentration is derived from ice-core data (Etheridge et al., 1996) and atmospheric measurements obtained at Maona Loa, Hawaii (Keeling et al., 1995). The model is run on a global quasi-1-degree equal-area grid with 10 525 non-glaciated land grid points. The grid has a resolution of 1 degree latitude by 1 degree longitude at the equator, with the same spacing along lines of equal latitude when away from the equator.

ACPD
12, 4243–4278, 2012

In variation to the standard LPJ-GUESS model, fire-related mortality is computed on a monthly time step by burning each patch with a probability equal to the observed burned fraction of the corresponding grid cell. If a patch burns, a random fraction of the cohorts representing woody PFTs is killed, where the average number of cohorts killed equals the PFT-dependent fire related mortality (see Table 1). Grasses are not killed in a fire but are assumed to re-sprout.

Fuel is represented by four classes: live grass, herbaceous litter (dead grass, leaves or needles), live tree leaves or needles, and woody litter (i.e. dead stems and branches). Following Lehsten et al. (2009), plant litter, if not consumed by fire, decomposes at differential rates, with a turnover time at 10 °C of 20 yr for woody litter (Weedon et al., 2009), but 2.83 yr for herbaceous litter as in (Sitch et al., 2003). Based on extensive observations by Shea et al. (1996), we assume that in each burned patch, 100 % of live grass and herbaceous litter of the fire affected patches burn, as well as 66 % of tree leaves.

We define the combustion factor of total simulated dead wood, c_w, the fraction of total dead woody plant material consumed in a fire, by:

$$c_w = c_{wl}(1 - f_{st}), \quad (1)$$

where f_{st} is the fraction of woody litter in dead standing trees, and c_{wl} the combustion factor of woody litter on the ground. The average combustion factor of woody litter reported by Shea et al. (1996) was 40 % across 12 sites, but ranged from 3 to 100 %. For one broad geographic location that comprises three of the sites (Kasanka, described as "moist savanna"), we performed a number of simulations with LPJ-GUESS. Simulated vegetation was roughly in-line with observations, but simulated woody litter was much higher. We attribute this to the fact that woody litter in LPJ-GUESS comprises both woody debris on the ground and wood in standing dead trees. Unfortunately, lack of ground data for f_{st} makes the task of assigning a plausible range for c_w difficult. Here, we simply use $c_{wl} = 0.4$ and vary f_{st} between 0 and 0.8, yielding a range for c_w from 0.08 to 0.4. We do not modify LPJ-GUESS to represent standing dead wood, but use c_w as the combustion factor for all woody litter and vary it between 0.08 and 0.40.

ACPD
12, 4243–4278, 2012

The standard LPJ-GUESS model treats leaf, stem and branch turnover at annual time steps. In order to realistically simulate seasonal variations of fuel load, input of dead leaves into the pool of herbaceous litter and the phenology of tropical raingreen trees have been modified according to Lehsten et al. (2009). For summergreen trees, the revised model uses length of day to predict the date of leaf shedding (White et al., 1997), set to the first day with length less than 10 h, or after 270 days after leaf shooting when day length is never less than 10 h. In the autumn, a day length of 10 h occurs between 21 October (Hainich, Germany, deciduous forest, latitude 51.0°) and 23 November (Goodwin Creek, Mississippi, deciduous forest, latitude 34.3°), the approximate latitude range where summergreen trees typically grow. The dates coincide with the time of declining vegetation greenness seen in satellite data for these two sites (http://fapar.jrc.ec.europa.eu/; Gobron et al., 2007). For grasses, the soil moisture triggers of the phenology scheme have also been modified similar to raingreen trees: leaf shoot requires that conditions have been wet for 7 days, while dry conditions for 30 days are sufficient to trigger leaf senescence.

2.2 Burned area data sets

We use three global multi-annual data sets of burned area: the global fire emissions data (GFED) version 3 burned area product, a monthly multi-sensor merged product starting in July 1996 and currently ending December 2010 (Giglio et al., 2010), the Moderate Resolution Imaging Spectroradiometer (MODIS) MCD45 burned area product based solely on the series of MODIS sensors, from April 2000 until November 2010 and a gap in June 2001 (Roy et al., 2005), and the L3JRC burned area product based on the SPOT-VEGETATION sensor starting April 2000 and ending March 2007 (Tansey et al., 2008). MCD45 reports up to one burning event per month and grid cell with an accuracy of several days, while L3JRC reports the date of up to one burning event per pixel for the season starting in April and ending in March the following year. From 2001 onwards, GFED3 uses mainly MODIS reflectance data as input, the same as MCD45. All three data sets were aggregated, if necessary, to 0.5 by 0.5 degree spatial

ACPD
12, 4243–4278, 2012

resolution, converted to monthly burned fraction of each grid cell and used as input to the modified LPJ-GUESS model. The gap in June 2000 for MCD45 was filled by using the average burned area for June of all the other years in the data set.

2.3 Emission models

The standard approach to modelling emissions from wildfires, established by Seiler and Crutzen (1980), is to assign emission factors converting combusted biomass to emissions of chemical species, with different emission factors for different ecosystems. Here, we use the latest compilation of such emission factors by Andreae and Merlet (2001), updated according to P. Merlet (personal communication, 2008) as Emissions Model 1 (EM1). Emission factors are given in g species per kg dry mass combusted. To convert output from LPJ-GUESS to dry matter, we assume a carbon content of 50 % for all dry, dead biomass (Ragland and Aerts, 1991). Separate emission factors are given for savanna and grassland, tropical forest, and extra-tropical forest. We assign these emission factors according to the vegetation simulated in LPJ-GUESS by using the following scheme: the category "savanna and grassland" is defined where the simulated fraction of grass LAI over total LAI is greater than 20 %, "tropical forest" where this fraction is less than 20 % and the dominant simulated PFT is a tropical tree, and "extra-tropical forest" when none of the other conditions is met. EM1 is used to simulate emissions of CO_2, CO, CH_4, non-methane hydrocarbons (NMHCs), total particulate matter (TPM), particulate matter of 2.5 micron and smaller diameter ($PM_{2.5}$), NO_x, N_2O, NH_3, SO_2, organic carbon (OC), black carbon (BC), ethane, propane, C_4 and higher alkanes, ethene, propene, C_4 and higher alkenes, methanol, ethanol, formaldehyde, acetaldehyde, acetone, benzene, toluene, and xylenes.

An alternative approach to using ecosystem type for differentiating between different emission factors is to model the modified combustion efficiency (MCE) and establish MCE-dependent emission factors. The MCE is defined as the amount of carbon emitted as CO_2 divided by the sum of carbon emitted as CO and CO_2. In Emissions Model 2 (EM2), MCE is computed from a linear function of the ratio of combusted woody

ACPD
12, 4243–4278, 2012

to grass litter, derived from the data presented by Ward et al. (1996). We decided against using the original non-linear model by Ward et al. (1996), because it predicts MCE = 0.85 when all litter is woody, which is much lower than the lowest ecosystem-specific value implied by the data of Andreae and Merlet (2001), which is 0.94 for extra-tropical forests. Also, Ward et al. (1996) present no data for a woody litter fraction greater than 0.84 (see Fig. A1). The original model by Ward et al. (1996) is based on fuel present at the sites, not the amount of fuel burnt in each fire. To obtain the amount of combusted fuel from the data by Ward et al. (1996), we assume that all grass present at the site burns completely, which is supported by a combustion factor of 1.0 for one site where almost all fuel is grass. It is also assumed that the combustion factors of all other fuel types than grass are the same. To obtain combusted woody litter, the combustion factor for fuel other than grass is then calculated from the reported total combustion factor using the equation $C_{ng} \cdot (T' - G') + G' = C \cdot T'$, where C is total combustion factor, C_{ng} non-grass combustion factor, T' total fuel present, and G' grass fuel present. We then use $L = C_{ng} \cdot L'$ and $G = G'$ to obtain combusted woody litter, L, and combusted grass, G, from woody litter (L') and grass (G') present at the site.

The linear model of the modified combustion efficiency derived from combusted fuel amounts is:

$$\mathrm{MCE} = 0.898 + 0.062 \cdot G/(G + L). \quad (2)$$

Emissions factors as a function of MCE are taken from Ward et al. (1996) for CO, CH_4, NMHCs and $PM_{2.5}$. The equation for NMHCs has been taken from Ward (2001), who cites Ward et al. (1996).

We use two further models for the emission of $PM_{2.5}$ based on (Janhäll et al., 2010). Emissions Model 3 (EM3) uses a linear relationship between the emission factor for particle mass and MCE taken from eq. 10 of Janhäll et al. (2010), using the MCE from EM2. The emissions factor for EM3, in g per kg dry mass, is:

$$\mathrm{EF}_{\mathrm{PM}_{2.5}} = 86.1 - 85.3 \cdot \mathrm{MCE} \pm 3.1 \quad (3)$$

ACPD
12, 4243–4278, 2012

The data for particle mass used by Janhäll et al. (2010) to derive Eq. (4) are for a maximum particle size of either 1 or 2.5 microns, with the majority falling into the $PM_{2.5}$ category. They report a small impact of using different size classes on their results.

Emissions Model 4 (EM4) uses fixed emission factors for aerosol mass differentiated between forest, savanna and grass biomes (Janhäll et al., 2010, Table 4). The values are 11 ± 6, 6 ± 3 and 5 ± 2 g per kg dry mass, respectively. For EM4, the three biomes are determined from the simulated grass fraction of LAI as follows: "forest" for up to 20 %, "savanna" for greater than 20 % and up to 80 %, and "grass" for greater than 80 %.

2.4 Uncertainties

Uncertainties in simulated emissions result from uncertainties in burned area, in the amount of combusted biomass on the burned surfaces, from differences between emissions models, and from the uncertainties of the emissions factor for a given model. To estimate uncertainty of emissions as a result of burned area, we use the sample standard deviation for the three simulations with different burned area products (using $N-1$ in the denominator). We use the same for $PM_{2.5}$ for the four emissions models, whereas for other species, where only two models are available, we indicate the range between the high and the low estimate. For uncertainties in combusted biomass, we use the range between the simulated values with a woody biomass combustion factor of 0.08 and 0.4. While two to four samples are certainly too few to derive a robust margin of error, this study nevertheless attempts to derive a first estimate of the contrasting contributors to uncertainties of wildfire chemical emissions.

To estimate the uncertainties resulting from the finite sample size of emissions factors measured in the field, we use the standard deviations of EM1 as reported by P. Merlet (personal communication, 2008), with the following provisions: if error margins are not given (only one or no measurements), we use twice the higher relative standard deviation of the other emission factor for the same species, as far as available, else four times the mean value. If uncertainties are given as a range (when only

ACPD
12, 4243–4278, 2012

two measurements are available), we use twice the range. We further assume that the uncertainties of emission factors for different ecosystems are uncorrelated in order to derive spatial integrals of uncertainty.

3 Results

3.1 Sensitivity to combustion factor and fuel load

A set of nine global simulations was performed with the ecosystem model LPJ-GUESS, first varying the combustion factor for woody litter (c_w), then the burned-area input data (see Table 2). The dependence of total global wildfire emissions in $TgC\,yr^{-1}$ – independent of chemical species, computed before the application of one of the emissions models – is shown in Fig. 1. In the plausible range of c_w of 0.08 to 0.4, fire emissions approximately double for both Africa and the remaining part of the globe.

The combustion factor for herbaceous fuel, here taken as 100 %, is generally better constrained than that for woody fuel and usually lies in the range of 95 to 100 % (Shea et al., 1996). The contribution of herbaceous fuel can be inferred from Fig. 1 at the point $c_w = 0$: emissions from herbaceous litter contribute about half (at $c_w = 0.08$) to one third ($c_w = 0.4$) of global emissions.

The importance of woody litter combustion can also be inferred from the global average amount of woody and herbaceous litter present at the burning sites. A global average for 1997–2009 of both litter types weighted by burned area in each grid cell yields $222\,gC\,m^{-2}$ herbaceous and $1730\,gC\,m^{-2}$ for woody litter, implying an average annual combusted amount of $222\,gC\,m^{-2}$ herbaceous litter and between 138 and $692\,gC\,m^{-2}$ woody litter, depending on c_w. Since uncertainties in the combustion factor of herbaceous fuel are much smaller than for woody fuel, we infer that simulated emissions are far more sensitive to uncertainties in woody than in herbaceous fuel combustion factors.

ACPD
12, 4243–4278, 2012

We also find that the value of $c_w = 0.2$ (Simulation 3 of Table 2) with GFED3 burned area gives results that are closest to the emissions estimates of GFED3 (Fig. 1). This value of 0.2 is retained throughout the remainder of this text and for further sensitivity analyses, where dependence of emissions of chemical species on burned area observations or emissions model are considered.

Another way of assessing the impact of different combustion factors and fuel loads is to compare the simulated emissions with GFED3 burned area and EM1 with those computed by van der Werf et al. (2010), who used the same burned area data and emissions model. While LPJ-GUESS simulates the vegetation present at each site as natural vegetation, the CASA model as used by van der Werf et al. (2010) uses observed vegetation distribution as an external input to the model. CASA also includes peat fires, deforestation and agricultural waste burning explicitly, while LPJ-GUESS simulates all observed fires as wildfires with no live biomass burned. In the case of deforestation fires, this leads to an underestimate of emissions because felling and burning of trees is not simulated. Table 3 shows the LPJ-GUESS and GFED3 CO emissions for wildfires and agricultural burning, and as well as total emissions for GFED3. For a definition of the regions see (Giglio et al., 2010) and Fig. B1.

Global emissions are 33 % higher for LPJ-GUESS compared to GFED3, about equal for Northern Hemisphere Africa, and 30 % higher for Southern Hemisphere Africa. Boreal North America is again higher by 43 %, while Boreal Asia is in close agreement. Southeast and Equatorial Asia are again somewhat higher for LPJ-GUESS when only considering wildfires and agricultural burning, but here the GFED3 total emissions are much higher due to the contribution from peat fires. The region that stands out in this comparison is Central Asia, where LPJ-GUESS emissions are an order of magnitude higher than GFED3. As Fig. 2 reveals, the region (see Fig. A2) has high simulated CO emissions especially in regions known to be dominated by agricultural fields (Ramankutty and Foley, 1999). One explanation for the discrepancy in emissions is that LPJ-GUESS simulates only potential natural vegetation, leading to overestimated fuel loads. This also explains why Europe and Temperate North America have much higher

ACPD
12, 4243–4278, 2012

simulated emissions for LPJ-GUESS. There is, however, reasonable agreement for the major emission regions, such as Africa, Australia, and South America.

3.2 Sensitivity to burned area

Not surprisingly, the spatial patterns of simulated wildfire emissions are dominated by the spatial patterns of the burned area product used. As GFED3 is mainly based on MODIS data from early 2000 onwards, those spatial patterns fall into two groups, with MODIS MCD45 and GFED3 as one, and L3JRC as the other (see Fig. 2 for the example of CO). A regional breakdown of the emissions (Table 3) also shows great similarity between GFED and MODIS, with the exception of some areas with minor contributions: Equatorial Asia, notably Boreal North America, where MODIS is close to half of GFED3, and Europe and Southeast Asia where this difference is reverted. The different burned area for Equatorial Asia was already noted by Giglio et al. (2010), where GFED3 reports generally much higher area burned. This was attributed to a mapping algorithm more resistant to cloud and aerosol contamination, leaving fewer undetected burning pixels.

With a much different burned area detection algorithm than GFED3 or MODIS MCD45 (Tansey et al., 2008; Roy and Boschetti, 2009; Giglio et al., 2010), the L3JRC product produces much higher emissions in the mid to high latitudes (Boreal and Temperate North America, Europe, Boreal and Central Asia; Table 3). The differences are by order of magnitude of emissions, as opposed to the much smaller differences between the two MODIS or predominantly MODIS-based products. For Africa, however, L3JRC based emissions are somewhat lower than MODIS or GFED3 emissions, which corresponds again to lower burned area in the region (Roy and Boschetti, 2009). MODIS and GFED3, on the other hand, are again very similar for this region. The general and substantial shift of emissions from the tropics to the high latitude going from GFED3 to L3JRC is also evident in Fig. 2. A further comparison shown in Fig. 3 reveals not only large differences in magnitude but also in interannual variability between simulations with different burned area data. For example, for Africa (Fig. 3b), interannual

ACPD
12, 4243–4278, 2012

variability is much larger for MODIS than for GFED3 burned area. For L3JRC, even temporal maxima and minima change sign compared to the other products: note for example that 2005 for Africa is a minimum for L3JRC, and a maximum for the other cases, or 2002 in the boreal zone, which is a pronounced temporal minimum in L3JRC, but not for any of the other data sets (Fig. 3a). On a global scale (Fig. 3c), GFED3 and MODIS lead to very similar results, however, with L3JRC standing out as much higher. The difference between GFED3 emissions and emissions from LPJ-GUESS with GFED3 burned area for 1997 can be attributed again to peat fires, which were especially wide-spread during the 1997/1998 El Niño (Page et al., 2002; Langenfelds et al., 2002).

3.3 Emissions models

Simulated emissions are found to be rather sensitive to the choice of emissions model, as is shown in Fig. 4. Annual carbon emissions for EM1 are 6655 Tg CO_2 (92.9 % of carbon emissions), 315 Tg CO (6.8 %), 14 Tg methane (0.5 %) and 18 Tg non-methane hydrocarbons (0.6 %), whereas for EM2 the figures are 8886 Tg CO_2 (90.4 %), 415 Tg CO (8.6 %), 15 Tg methane (0.6 %), and 15 Tg NMHCs (0.4 %). (The calculation assumes an average molar mass per carbon atom of 20 g for NMHCs derived from the data by P. Merlet (personal communication, 2008) for tropical grasslands and savannas.) EM2 thus predicts a considerably lower combustion efficiency for wildfires with much higher CO emissions, while EM1 yields a smaller combustion efficiency, but with fires producing considerably more NMHCs relative to methane.

In general, the choice of emissions model impacts more the magnitude and less the geographical breakdown of emissions (Fig. 4). At least for CO and methane, the share of emissions going to Africa is somewhat higher for EM2 (CO: 56 %, methane: 55 %) than for EM1 (CO: 52 %, methane: 51 %). For aerosols ($PM_{2.5}$), there are some notable redistributions in emissions: For EM4, most emissions come from Africa (60 %) and Southeast Asia and Oceania (11 %), with the boreal zone and temperate zones only contributing 10 % each. EM1, at the other end of the spectrum, allocates only 47 % to

ACPD
12, 4243–4278, 2012

Africa, but 18 % each to the boreal and temperate zones, and only 8 % to Southeast Asia and Oceania. We further find that choice of emissions model generally has only a small effect on interannual variations of emissions (results not shown).

3.4 Contributions to emissions uncertainties

We compare our best-guess estimate of global chemical emissions, for which we use EM1, $c_w = 0.2$ and GFED3 burned area, with uncertainty ranges resulting from uncertainties in emissions factor, emissions model, fuel combustion, or burned area (Table 4; see Sect. 2.4). Since this is only a first attempt at characterizing uncertainty ranges of chemical emissions from wildfires, we do not include an estimate of overall uncertainty, nor do we base our best guess on the average across emission models and burned area products.

In general, emissions factor uncertainties have a smaller impact on simulated emissions than either the simulated amount of combusted fuel, or the burned area. Differences between emissions models have a similar impact to uncertainties in emissions factors themselves, at least for the five cases where more than one model was available. The other important result is that the simulated amount of fuel combustion in a fire has a similar impact on uncertainties as the burned area itself. We find this for all simulated species.

On the other hand, there are cases where emission factor uncertainty has a similar or larger impact on emissions than any of the other factors. The tracers where the estimated impact exceeds that of fuel combustion are propane, SO_2, xylenes and ethanol. Propane has a much higher emissions factor for tropical forest (1.04 kg g^{-1} dry matter, P. Merlet, personal communication, 2008) than for savanna and grassland (0.086) or extratropical forest (0.27), but this high factor for tropical forests is based on only two measurements. Xylenes have the highest estimated emission factor for extratropical forest (0.2) based on only one measurement (vs. 0.043 and 0.087 for the other biomes), and ethanol has only one measurement for extratropical forest and none for the other ecosystems. Other cases with relatively large uncertainties due to emissions

ACPD
12, 4243–4278, 2012

factors are NO_x, NH_3, ethene, propene, benzene, toluene, methanol, formaldehyde, acetaldehyde and acteone.

For CO_2, uncertainties are determined almost exclusively by fuel combustion or burned area. This is because the relative uncertainty in combustion efficiency is much smaller than the relative uncertainty in the emissions factor of all remaining species. We find a remarkably large difference between the two emissions models for CO, resulting in a range of 100 Tg yr^{-1}, twice as much as the effect of the uncertainty of the emissions factor in EM1. Taking both emission factor and emission model uncertainty together and assuming they are uncorrelated yields the following overall result: the uncertainties of the five main groups of emitted species (CO_2, CO, CH_4, NHMCs and particulate matter) have about 50 % (CO_2) to 75 % estimated uncertainty from fuel combustion or burned area, and about 20 to 30 % from emissions modelling, except for CO_2 (5 %) and CO (36 % from emissions modelling).

4 Discussion

Even though some of the results have been presented in terms of uncertainties, it must be stressed that the reported ranges are only a first estimate. This estimate has been derived from what is essentially a sensitivity analysis of chemical emissions from wildfires to plausible scenarios of parameter, model or input data choice. The first issue to discuss is therefore how the models used here compare with other global modelling efforts of wildfire emissions.

As for combustion factors, Ito and Penner (2004) used values for herbaceous and fine litter fuels of 0.99 for forested areas and between 0.44 and 0.98 for grasslands. Wiedinmyer et al. (2006) used 0.9 for forested areas and 0.98 for grasslands. If we change the combustion factor of 1 for herbaceous fuel to 0.7, which is the average of the range used by Ito and Penner, the average combusted herbaceous fuel changes from 222 to 155 gC m^{-2}. The amount of change is only 3 % of the average simulated fuel load of to 1952 gC m^{-2}. Even though these calculations are only approximate, because changing

ACPD
12, 4243–4278, 2012

the combustion factor will slightly change the simulated fuel amount, we conclude that neglecting the sensitivity of simulated emissions on fine and herbaceous fuel combustion factors is justified.

A review of combustion factors for coarse fuel by Ito and Penner (2004) showed a mean value of 0.27 ± 0.09 (one standard deviation). Taking twice the standard deviation yields a plausible range for this value of 0.09 to 0.45, rather close to the range used here for c_w (0.08 to 0.4). We must note, however, that other uncertainties are represented only by one standard deviation. Therefore, the range taken for c_w might over-represent the impact of uncertainties in combustion factors alone. However, total combusted biomass also depends on the simulated amount of fuel, which depends on simulated type and amount of vegetation, and the turnover time of the different litter types.

We find that the simulated amount of woody litter from LPJ-GUESS (in dry mass per m^2) is reasonably close to cited values: 0.15 kg for grassland, 5.5 kg for savannas and 15 kg for forests (using the same definitions as EM4), against 0.09 kg for grasslands, 1.7 kg for open shrublands, and 8.0–14.3 kg for forests as compiled by Ito and Penner (2004). Their value for herbaceous fuel in grasslands, 1.0 kg, is also similar to the average simulated value by LPJ-GUESS of 0.9 kg. This comparison is based on LPJ-GUESS simulations with $c_w = 0.2$ and GFED3 burned area averaged over 1997 to 2009. Using $c_w = 0.08$ or 0.4 increases or decreases simulated average woody litter by approximately 10 % for savannas, and 2 % for forests.

While simulated fuel amounts seem reasonable, we have to expect that different parameterisations of litter turnover or different vegetation dynamics will result in substantial variations in simulated fuel loads, and thus further contribute to uncertainties in simulated chemical emissions from wildfires. The additional uncertainty of the simulated combusted biomass, however, can also be approximated by taking a larger range in c_w than would be expected from uncertainties in the woody combustion factors alone. As noted before, the range used here for c_w is about twice as large as the range for the combustion factor of coarse fuel by Ito and Penner plus or minus one standard

ACPD
12, 4243–4278, 2012

deviation. Because other uncertainties are represented by one standard devation, the results reported here (Table 4 under "fuel combustion") can be taken as a reasonable representation of the effect of uncertainties in the simulated amount of combusted fuel due to various factors.

For the sensitivity to emissions factors we used ranges defined by one standard deviation reported by P. Merlet (personal communication, 2008). Whether these ranges represent the plausible range of emissions factors can be addressed by comparing results with different emissions models against the propagation of uncertainties in emissions factors. We find that propagation of uncertainties might somewhat underestimate the impact of varying emissions factors within a full plausible range, in one case (CO) even substantially. However, we need to remember that the model of MCE used in EM2 was derived from data from African savannas only and might be less applicable in e.g. boreal forests. We therefore assume that the sensitivity of emissions to emission models can be reasonably approximated by varying the emission factor within the reported one standard deviation of the mean. However, we must also note that using a more process based model of emission factors, as presented by van Leeuwen and van der Werf (2011), it might become possible to narrow down emissions factors, if it turns out that other factors than fuel composition or biome are better predictors.

The remaining question is whether the rather wide range of spatial patterns of burned area used in this study, with large differences between two predominantly MODIS based products and L3JRC, can be considered a plausible range of either observed or simulated burned area. A striking feature of the L3JRC product is the very high burned area in the boreal zone compared to the other products. A comparison by Giglio et al. (2010) against national fire data by the USA and Canada showed much better agreement for GFED3 than MODIS MCD45, with MCD45 underestimating substantially in Canada and Alaska, but with L3JRC up to an order of magnitude higher than the national data. On the other hand, GFED3 and MCD45 are very similar in Africa, where more than half of the emissions originate. Using the sample standard deviation over three products already gives twice the weight to the predominantly MODIS based

ACPD
12, 4243–4278, 2012

products. We therefore believe that the use of the three products to estimate a plausible range of burned area is reasonable on a global scale, and the result justified that the sensitivity to differences in burned area is about as large as that to fuel combustion. For a regional analysis, however, it would be desirable to include regional data sets, which may be more reliable than the global remote sensing based products.

Returning to the initial question about the possibility of future projections of chemical emissions from wildfires, it appears that there is first of all need for clarifying which observed burned area products are the most reliable and should be used for model testing. While the very high emissions in the boreal zone of L3JRC might well be an outlier, a comprehensive intercomparison of regional and global burned area products seems highly desirable. As far as modelling burned area is concerned, the results from global fire models are promising, but their application remains a substantial challenge. For example, Thonicke et al. (2010) report fractional area burned in southern Europe and Turkey similar to African savannas. In GFED3 only central Portugal has areas with values between 5 and 10 % yr^{-1}, with the rest of the region closer to 1 % yr^{-1}. By comparison, African savannas burn between 10 and 30 % of its area each year. While the model by Thonicke et al. (2010) is more process based, Kloster et al. (2010) show results of simulated burned area using the much simpler approaches of Thonicke et al. (2001) and Arora and Boer (2005) and find reasonable broad agreement with L3JRC and GFED2 (Giglio et al., 2006). However, Giglio et al. (2010) found that GFED3 agrees substantially better with independent data than either GFED2 or L3JRC. This has consequences for model evaluation: for example, the model by Arora and Boer (2005) simulates twice to 6 times the GFED2 burned area for Europe, and GFED3 has 75 % less burned area in the same region than GFED2 (Giglio et al., 2010).

Overall, we find that in order to arrive at a predictive capability for the impacts of climate change on wildfire emissions, the main priority is to obtain more data on combustion factors and in particular factors that allow determination of the associated burn conditions, as the currently available data serious limits modelling capability (Ito and Penner, 2004; Wiedinmyer et al., 2010). The next highest priority would be a systematic

ACPD
12, 4243–4278, 2012

comparison of global and regional data on burned area, and a systematic improvement of burned area models to better match well-validated observations. Finally, the range of emissions reported here could be tested against atmospheric observations of relatively long-lived chemical tracers such as CO (in combination with Chemistry-Transport Models), to establish whether these can be used to provide constraints especially in regions with large differences in simulated emissions, such as the boreal zone.

5 Conclusions

We have presented a framework for exploring the sensitivity of global chemical emissions from wildfires to various uncertain model inputs and parameterisations. While showing that global burned area modelling and lack of data on combustion factors and the fate of woody debris in a fire are major concerns, the study also highlights the need for better models of emission factors for several species. For the main emitting species, however, the main issue is accurate modelling of burned area and combusted biomass, crucial for assessing fire emissions in past or future environments.

Our results can be used by the atmospheric modelling community to consider a range of emissions scenarios rather than a fixed one, reflecting the uncertainty range due to current modelling capabilities. In certain cases, modelling different emissions scenarios together with chemical transport could be used to further constrain emissions, given suitable observations and long-lived tracers.

We conclude that model-based prediction of chemical emissions from wildfire, either for present or future conditions, still carries a rather high degree of uncertainty.

All emissions fields presented are available on request by the corresponding author.

Acknowledgements. This work was supported by EU contracts 265148 (Pan-European Gas-Aerosol-climate interation Study, PEGASOS), and 243888 (Forest fires under climate, social and economic changes in Europe, the Mediterranean and other fire-affected areas of the world, FUME).

ACPD
12, 4243–4278, 2012

References

Andreae, M. O. and Merlet, P.: Emission of trace gases and aerosols from biomass burning, Global Biogeochem. Cy., 15, 955–966, 2001.

Arneth, A., Harrison, S. P., Zaehle, S., Tsigaridis, K., Menon, S., Bartlein, P. J., Feichter, J., Korhola, A., Kulmala, M., O'Donnell, D., Schurgers, G., Sorvari, S., and Vesala, T.: Terrestrial biogeochemical feedbacks in the climate system, Nat. Geosci., 3, 525–532, doi:10.1038/Ngeo905, 2010.

Arora, V. K. and Boer, G. J.: Fire as an interactive component of dynamic vegetation models, J. Geophys. Res., 110, G02008, doi:10.1029/2005jg000042, 2005.

Boschetti, L. and Roy, D. P.: Strategies for the fusion of satellite fire radiative power with burned area data for fire radiative energy derivation, J. Geophys. Res., 114, D20302, doi:10.1029/2008jd011645, 2009.

Bowman, D. M. J. S., Balch, J. K., Artaxo, P., Bond, W. J., Carlson, J. M., Cochrane, M. A., D'Antonio, C. M., DeFries, R. S., Doyle, J. C., Harrison, S. P., Johnston, F. H., Keeley, J. E., Krawchuk, M. A., Kull, C. A., Marston, J. B., Moritz, M. A., Prentice, I. C., Roos, C. I., Scott, A. C., Swetnam, T. W., van der Werf, G. R., and Pyne, S. J.: Fire in the Earth System, Science, 324, 481–484, doi:10.1126/Science.1163886, 2009.

Duncan, B. N., Martin, R. V., Staudt, A. C., Yevich, R., and Logan, J. A.: Interannual and seasonal variability of biomass burning emissions constrained by satellite observations, J. Geophys. Res., 108, 4100, doi:10.1029/2002jd002378, 2003.

Etheridge, D. M., Steele, L. P., Langenfelds, R., and Francey, R. J.: Natural and anthropogenic changes in atmospheric CO_2 over the last 1000 years from air in Antarctic ice and firn, J. Geophys. Res., 101, 4115–4128, 1996.

Gregoire, J. M., Tansey, K., and Silva, J. M. N.: The GBA2000 initiative: developing a global burnt area database from SPOT-VEGETATION imagery, Int. J. Remote Sens., 24, 1369–1376, doi:10.1080/0143116021000044850, 2003.

Giglio, L., van der Werf, G. R., Randerson, J. T., Collatz, G. J., and Kasibhatla, P.: Global estimation of burned area using MODIS active fire observations, Atmos. Chem. Phys., 6, 957–974, doi:10.5194/acp-6-957-2006, 2006.

Giglio, L., Randerson, J. T., van der Werf, G. R., Kasibhatla, P. S., Collatz, G. J., Morton, D. C., and DeFries, R. S.: Assessing variability and long-term trends in burned area by merging multiple satellite fire products, Biogeosciences, 7, 1171–1186, doi:10.5194/bg-7-1171-2010,

ACPD
12, 4243–4278, 2012

2010.
Gobron, N., Pinty , B., Melin, F., Taberner , M., Verstraete, M. M., Robustelli, M., and Widlowski, J.-L.: Evaluation of the MERIS/ENVISAT FAPAR product, Adv. Space Res., 39, 105–115, 2007.
Govaerts, Y., Pereira, J. M., Pinty, B., and Mota, B.: Impact of fires on surface albedo dynamics over the African continent, J. Geophys. Res., 107, 4629, doi:4610.1029/2002JD002388, 2002.
Hoelzemann, J. J., Schultz, M. G., Brasseur, G. P., Granier, C., and Simon, M.: Global Wildland Fire Emission Model (GWEM): Evaluating the use of global area burnt satellite data, J. Geophys. Res., 109, D14S04, doi:10.1029/2003jd003666, 2004.
Ito, A. and Penner, J. E.: Global estimates of biomass burning emissions based on satellite imagery for the year 2000, J. Geophys. Res., 109, D14S05, doi:10.1029/2003jd004423, 2004.
Janhäll, S., Andreae, M. O., and Pöschl, U.: Biomass burning aerosol emissions from vegetation fires: particle number and mass emission factors and size distributions, Atmos. Chem. Phys., 10, 1427–1439, doi:10.5194/acp-10-1427-2010, 2010.
Jones, P. D. and Harris, I.: CRU Time Series (TS) high resolution gridded datasets, NCAS British Atmospheric Data Centre, 2011.
Keeling, C. D., Whorf, T. P., Wahlen, M., and Vanderplicht, J.: Interannual extremes in the rate of rise of carbon dioxide since 1980, Nature, 375, 666–670, 1995.
Langenfelds, R. L., Francey, R. J., Pak, B. C., Steele, L. P., Lloyd, J., Trudinger, C. M., and Allison, C. E.: Interannual growth rate variations of atmospheric CO_2 and its $\delta^{13}C$, H_2, CH_4, and CO between 1992 and 1999 linked to biomass burning, Global Biogeochem. Cy., 16, 1048–1069, 2002.
Langmann, B., Duncan, B., Textor, C., Trentmann, J., and van der Werf, G. R.: Vegetation fire emissions and their impact on air pollution and climate, Atmos. Environ., 43, 107–116, 2009.
Lehsten, V., Tansey, K., Balzter, H., Thonicke, K., Spessa, A., Weber, U., Smith, B., and Arneth, A.: Estimating carbon emissions from African wildfires, Biogeosciences, 6, 349–360, doi:10.5194/bg-6-349-2009, 2009.
Matson, M. and Dozier, J.: Identification of Subresolution High-Temperature Sources Using a Thermal Ir Sensor, Photogramm. Eng. Rem. S, 47, 1311–1318, 1981.
Mieville, A., Granier, C., Liousse, C., Guillaume, B., Mouillot, F., Lamarque, J. F., Gregoire, J. M., and Petron, G.: Emissions of gases and particles from biomass burning during the 20th century using satellite data and an historical reconstruction, Atmos. Environ., 44, 1469–1477,

ACPD
12, 4243–4278, 2012

2010.
Mitchell, T. D. and Jones, P. D.: An improved method for constructing a database of monthly climate observations and associated high-resolution grids, Int. J. Climatol., 25, 693–712, 2005.
Mouillot, F. and Field, C. B.: Fire history and the global carbon budget: a 1 degrees × 1 degrees fire history reconstruction for the 20th century, Glob. Change Biol., 11, 398–420, doi:10.1111/J.1365-2486.2005.00920.X, 2005.
Page, S. E., Siegert, F., Rieley, J. O., Boehm, H.-D. V., Jayak, A., and Limink, S.: The amount of carbon released from peat and forest fires in Indonesia during 1997, Nature, 420, 61–65, 2002.
Prentice, I. C., Kelley, D. I., Foster, P. N., Friedlingstein, P., Harrison, S. P., and Bartlein, P. J.: Modeling fire and the terrestrial carbon balance, Global Biogeochem. Cy., 25, GB3005, doi:10.1029/2010gb003906, 2011.
Ragland, K. W. and Aerts, D. J.: Properties of wood for combustion analysis, Bioresource Technol., 37, 161–168, 1991.
Ramankutty, N. and Foley, J. A.: Estimating historical changes in global land cover: Croplands from 1700 to 1992, Global Biogeochem. Cy., 13, 997–1027, 1999.
Roy, D. P. and Boschetti, L.: Southern Africa Validation of the MODIS, L3JRC, and GlobCarbon Burned-Area Products, IEEE Trans Geosci Remote, 47, 1032–1044, doi:10.1109/Tgrs.2008.2009000, 2009.
Roy, D. P., Jin, Y., Lewis, P. E., and Justice, C. O.: Prototyping a global algorithm for systematic fire-affected area mapping using MODIS time series data, Remote Sens. Eviron., 97, 137–162, 2005.
Roy, D. P., Jin, Y., Lewis, P. E., and Justice, C. O.: Prototyping a global algorithm for systematic fire-affected area mapping using MODIS time series data, Remote Sens. Eviron., 97, 137–162, 2005.
Schultz, M. G.: On the use of ATSR fire count data to estimate the seasonal and interannual variability of vegetation fire emissions, Atmos. Chem. Phys., 2, 387–395, doi:10.5194/acp-2-387-2002, 2002.
Schultz, M. G., Heil, A., Hoelzemann, J. J., Spessa, A., Thonicke, K., Goldammer, J. G., Held, A. C., Pereira, J. M. C., and van het Bolscher, M.: Global wildland fire emissions from 1960 to 2000, Global Biogeochem. Cy., 22, GB2002, doi:10.1029/2007gb003031, 2008.
Seiler, W. and Crutzen, P. J.: Estimates of Gross and Net Fluxes of Carbon between the

ACPD
12, 4243–4278, 2012

Biosphere and the Atmosphere from Biomass Burning, Climatic Change, 2, 207–247, 1980.
Shea, R. W., Shea, B. W., Kauffman, J. B., Ward, D. E., Haskins, C. I., and Scholes, M. C.: Fuel biomass and combustion factors associated with fires in savanna ecosystems of South Africa and Zambia, J. Geophys. Res., 101, 23551–23568, 1996.
Simon, M., Plummer, S., Fierens, F., Hoelzemann, J. J., and Arino, O.: Burnt area detection at global scale using ATSR-2: The GLOBSCAR products and their qualification, J. Geophys. Res., 109, D14S02, doi:10.1029/2003jd003622, 2004.
Sitch, S., Smith, B., Prentice, I. C., Arneth, A., Bondeau, A., Cramer, W., Kaplan, J. O., Levis, S., Lucht, W., Sykes, M. T., Thonicke, K., and Venevsky, S.: Evaluation of ecosystem dynamics, plant geography and terrestrial carbon cycling in the LPJ dynamic global vegetation model, Glob. Change Biol., 9, 161–185, 2003.
Smith, B., Prentice, C., and Sykes, M.: Representation of vegetation dynamics in modelling of terrestrial ecosystems: comparing two contrasting approaches within European climate space, Global Ecol. Biogeogr., 10, 621–637, 2001.
Tansey, K., Gregoire, J. M., Defourny, P., Leigh, R., Pekel, J. F. O., van Bogaert, E., and Bartholome, E.: A new, global, multi-annual (2000–2007) burnt area product at 1 km resolution, Geophys. Res. Lett., 35, L01401, doi:10.1029/2007gl031567, 2008.
Thonicke, K., Venevsky, S., Sitch, S., and Cramer, W.: The role of fire disturbance for global vegetation dynamics: coupling fire into a Dynamic Global Vegetation Model, Global Ecol. Biogeogr., 10, 661–677, 2001.
Thonicke, K., Spessa, A., Prentice, I. C., Harrison, S. P., Dong, L., and Carmona-Moreno, C.: The influence of vegetation, fire spread and fire behaviour on biomass burning and trace gas emissions: results from a process-based model, Biogeosciences, 7, 1991–2011, doi:10.5194/bg-7-1991-2010, 2010.
van der Werf, G. R., Randerson, J. T., Giglio, L., Collatz, G. J., Kasibhatla, P. S., and Arellano Jr., A. F.: Interannual variability in global biomass burning emissions from 1997 to 2004, Atmos. Chem. Phys., 6, 3423–3441, doi:10.5194/acp-6-3423-2006, 2006.
van der Werf, G. R., Randerson, J. T., Giglio, L., Collatz, G. J., Mu, M., Kasibhatla, P. S., Morton, D. C., DeFries, R. S., Jin, Y., and van Leeuwen, T. T.: Global fire emissions and the contribution of deforestation, savanna, forest, agricultural, and peat fires (1997–2009), Atmos. Chem. Phys., 10, 11707–11735, doi:10.5194/acp-10-11707-2010, 2010.
van Leeuwen, T. T. and van der Werf, G. R.: Spatial and temporal variability in the ratio of trace gases emitted from biomass burning, Atmos. Chem. Phys., 11, 3611–3629, doi:10.5194/acp-

ACPD
12, 4243–4278, 2012

11-3611-2011, 2011.
Ward, D.: Combustion chemistry and smoke, in: Forest Fires – Behavior and Ecological Effects, edited by: Johnson, E. A. and Miyanishi, K., Academic Press, San Diego, 55–77, 2001.
Ward, D. E., Hao, W. M., Susott, R. A., Babbitt, R. E., Shea, R. W., Kauffman, J. B., and Justice, C. O.: Effect of fuel composition on combustion efficiency and emission factors for African savanna ecosystems, J. Geophys. Res., 101, 23569–523576, 1996.
Weedon, J. T., Cornwell, W. K., Cornelissen, J. H. C., Zanne, A. E., Wirth, C., and Coomes, D. A.: Global meta-analysis of wood decomposition rates: a role for trait variation among tree species?, Ecol. Lett., 12, 45–56, 2009.
Wiedinmyer, C., Quayle, B., Geron, C., Belote, A., McKenzie, D., Zhang, X. Y., O'Neill, S., and Wynne, K. K.: Estimating emissions from fires in North America for air quality modeling, Atmos. Environ., 40, 3419–3432, 2006.
White, M. A., Thornton, P. E., and Running, S. W.: A continental phenology model for monitoring vegetation responses to interannual climatic variability, Global Biogeochem. Cy., 11, 217–234, 1997.
Wooster, M. J., Roberts, G., Perry, G. L. W., and Kaufman, Y. L.: Retrieval of biomass combustion rates and totals from fire radiative power observations: FRP derivation and calibration relationships between biomass consumption and fire radiative energy release, J. Geophys. Res., 110, D24311, doi:10.1029/2005JD006318, 2005.

ACPD
12, 4243–4278, 2012

Table 1. Plant functional types and fire-related mortality used with LPJ-GUESS.

PFT	Shade tolerant	Fire-related mortality
Boreal needle-leaved evergreen tree	x	0.7
Boreal needle-leaved evergreen tree		0.7
Boreal needle-leaved summergreen tree		0.7
Temperate broad-leaved summergreen tree	x	0.9
Temperate broad-leaved summergreen tree		0.9
Temperate broad-leaved evergreen tree	x	0.7
Tropical broadleaved evergreen tree	x	0.9
Tropical broadleaved evergreen tree		0.9
Tropical broadleaved raingreen tree		0.7
Cool (C3) grass		1.0
Warm (C4) grass		1.0

ACPD
12, 4243–4278, 2012

Table 2. Description of simulations performed with LPJ-GUESS.

Simulation	c_w^*	Burned-area data	Period of burned-area data
1	0	GFED3	9/1996–12/2009
2	0.08	”	”
3	0.2	”	”
4	0.4	”	”
5	1	”	”
6	0.2	MODIS MCD45	4/2000–12/2009
7	0.2	L3JRC	4/2000–3/2007

*Combustion factor for woody litter.

ACPD
12, 4243–4278, 2012

Table 3. Average annual CO emissions in Tg 2001–2006 with LPJ-GUESS and Emissions Model 1 using different remotely sensed burned area products: GFED3 (Giglio et al., 2010). L3JRC (Tansey et al., 2008), MODIS MCD45 (Roy et al., 2005). Last column are emissions by GFED3. Wildfires exclude deforestation, peat fires and agricultural waste burning (Agric.).

Model	LPJ-GUESS + EM1			GFED3*	
Burned area product	GFED3	MODIS	L3JRC	GFED3	
Types of fires	Wildfires + Agric. Fires			Wildf.+Agric.	All
Boreal North America	20.2	12.8	93.1	14.1	14.2
Temperate North America	4.2	5.9	53.1	1.5	1.5
Central America	1.6	1.7	4.6	1.8	3.3
Northern Hemisph. South America	2.8	2.4	3.6	1.9	3.5
Southern Hemisph. South America	26.5	24.0	37.1	17.9	48.7
Europe	1.5	3.5	26.9	0.8	0.8
Middle East	0.9	1.3	6.6	0.4	0.3
Northern Hemisphere Africa	60.5	62.2	41.5	60.0	67.8
Southern Hemisphere Africa	103.4	102.9	79.7	79.6	85.1
Boreal Asia	29.4	28.5	137.9	27.8	26.8
Central Asia	42.8	51.1	167.2	5.9	6.2
Southeast Asia	5.9	8.4	6.9	6.0	16.6
Equatorial Asia	1.8	0.4	0.2	1.8	50.1
Australia and New Zeeland	18.4	14.1	15.8	19.9	20.5
Global	319.9	319.3	674.0	239.2	346.3

* van der Werf et al. (2010)

ACPD
12, 4243–4278, 2012

Table 4. Global wildfire emissions in Tg yr^{-1} with Emission Model 1, $c_w = 0.2$ and GFED3 burned area (best guess), and uncertainties from various factors. "Higher alkenes" and "higher alkanes" with a least 4 C atoms. OC: organic carbon. BC: black carbon. NMHCs: non-methane hydrocarbons. TPM: total particulate matter.

Species	Best guess[1]	Uncertainty resulting from:			
		emission factor[1]	emission model[1]	fuel combustion[1]	burned area[2]
CO_2	6656	271	*230*	3959	3910
CO	315	50	*100*	206	205
CH_4	14.4	2.8	*0.9*	10.1	8.4
NMHCs	18.5	4.9	*3.5*	12.3	11.0
TPM	44.2	10.2	–	28.9	32.8
$PM_{2.5}$	29.3	6.8	3.6	20.0	22.3
NO_x	9.75	3.45	–	6.11	6.85
N_2O	0.89	0.30	–	0.54	0.58
NH_3	3.85	1.77	–	2.52	2.96
SO_2	2.26	3.09	–	1.55	1.70
OC	18.4	4.1	–	12.4	15.7
BC	2.04	0.52	–	1.26	1.26
ethene	4.20	1.43	–	2.72	2.44
ethane	2.24	0.65	–	1.60	1.24
propene	2.20	0.78	–	1.54	1.07
propane	1.25	2.82	–	0.99	0.38
higher alkenes	2.01	0.45	–	1.31	1.28
higher alkanes	0.78	0.19	–	0.54	0.61
benzene	1.40	0.57	–	0.91	1.00
toluene	0.95	0.46	–	0.62	0.72
xylenes	0.33	0.31	–	0.24	0.31
methanol	7.50	3.66	–	4.89	4.01
ethanol	0.05	0.06	–	0.03	0.03
formaldehyde	5.18	2.12	–	3.72	3.51
acetaldehyde	3.80	2.55	–	2.76	1.71
acetone	2.22	0.79	–	1.40	1.41

[1] 1997–2009, [2] 2001–2006. Range based on two samples shown in *italics.*

ACPD
12, 4243–4278, 2012

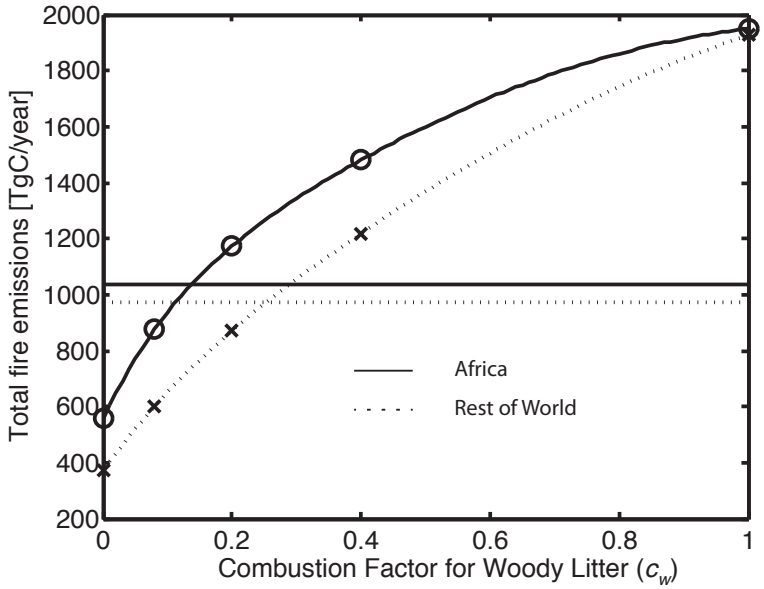

Fig. 1. Sensitivity of average global fire emissions 1997–2009. The horizontal lines show GFED3 emissions during the same period.

ACPD
12, 4243–4278, 2012

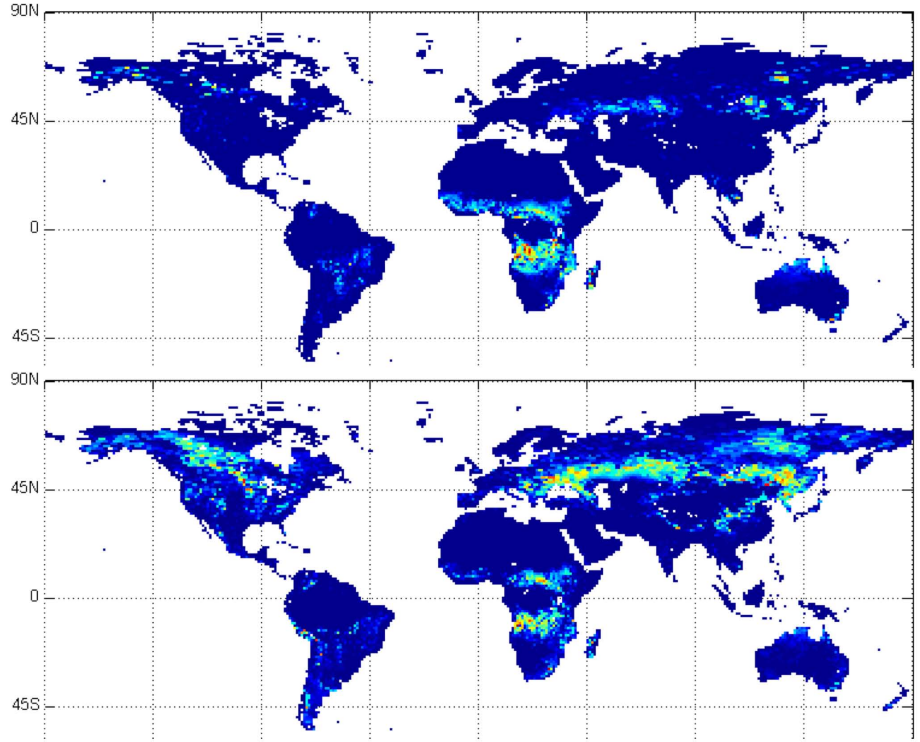

Fig. 2. CO emissions in gC m^{-2} yr^{-1} for $c_w = 0.2$ and Emissions Model 1, average 2001–2006. Upper panel: GFED3 burned area. Lower panel: L3JRC burned area.

ACPD
12, 4243–4278, 2012

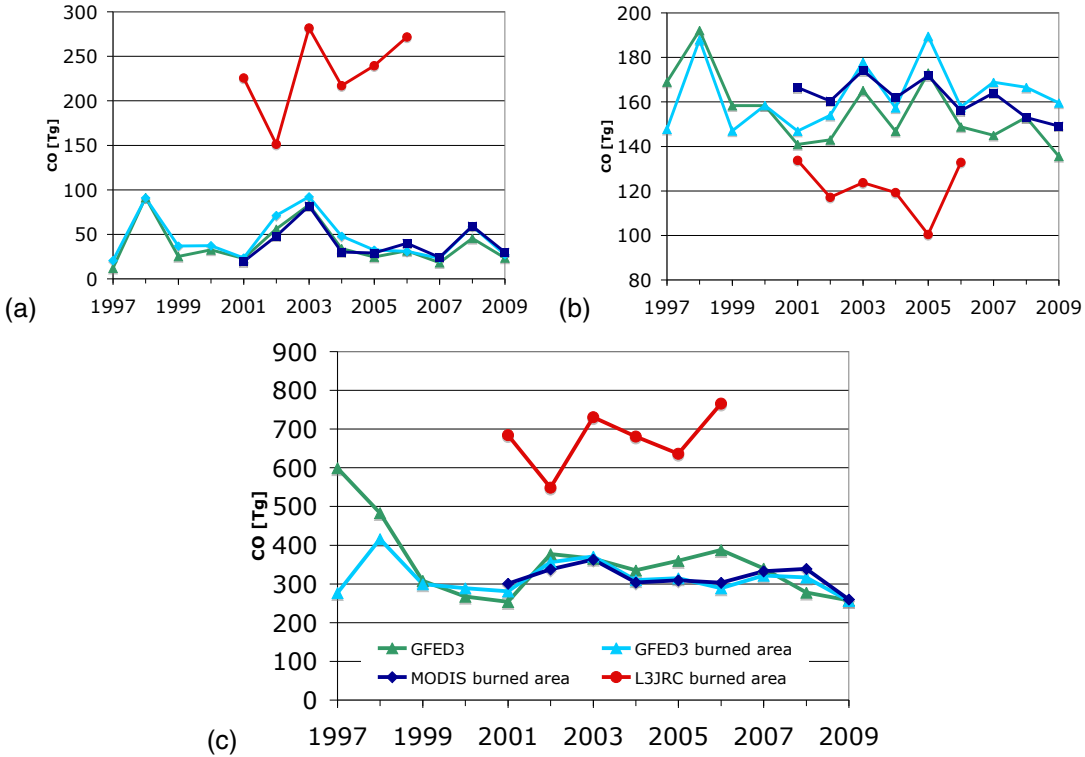

Fig. 3. Annual CO emissions in Tg for $c_w = 0.2$ and Emissions Model 1, for different burned area data sets, and total GFED3 emissions. **(a)** Boreal Asia and North America. **(b)** Africa. **(c)** Globe.

ACPD
12, 4243–4278, 2012

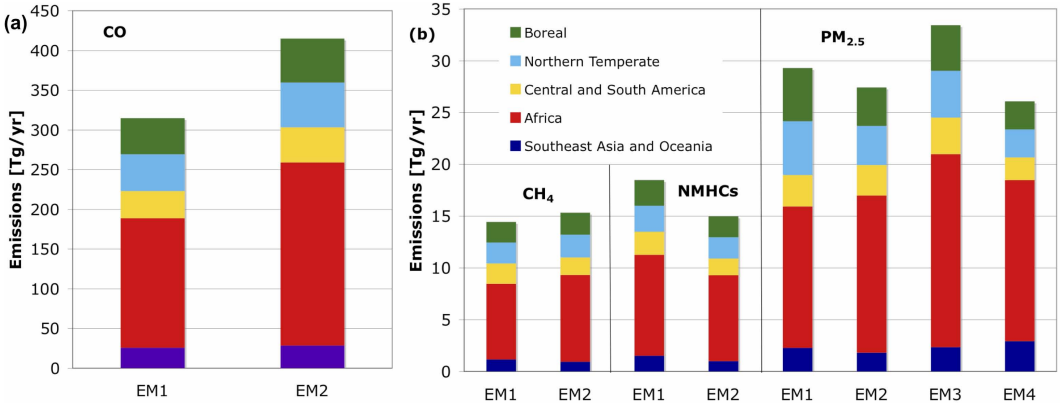

Fig. 4. Annual emissions in Tg by region of **(a)** CO; and of **(b)** methane, non-methane hydrocarbons (NMHCs) and aerosol particulate matter up to 2.5 microns, averaged 1997–2009. Emissions are for $c_w = 0.2$ and different emissions model (EM). Boreal: Boreal North America and Boreal Asia. Northern Temperate: Temperate North America, Europe, Middle East and Central Asia. Southeast Asia and Oceania: Southeast Asia, Equatorial Asia and Australia and New Zealand.

ACPD
12, 4243–4278, 2012

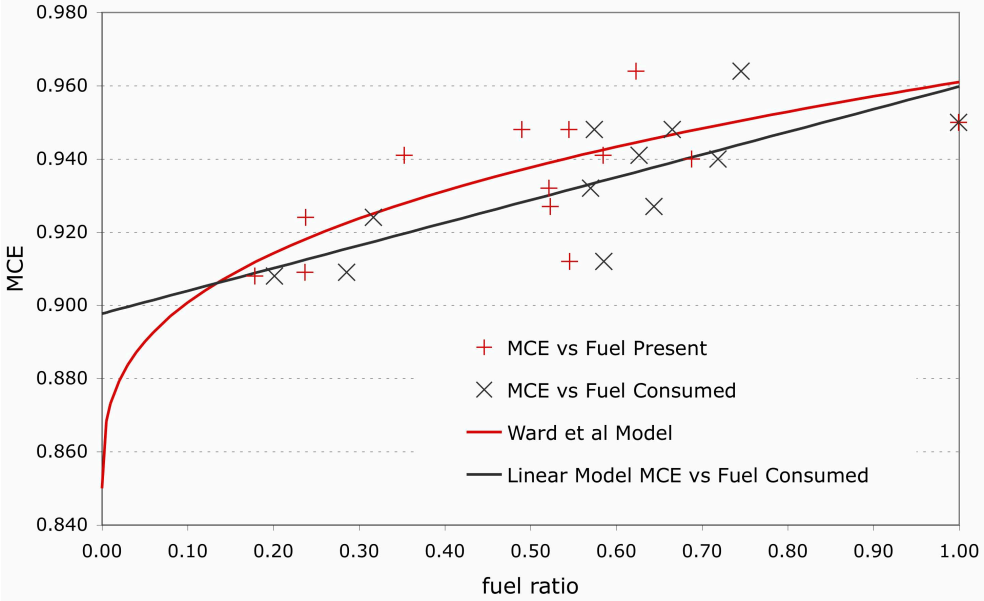

Fig. A1. Models of Modified Combustion Efficiency (MCE) against fuel ratio according to Ward et al. (1996) and derived as in the main text, as well as measured MCE by Ward et al. (1996) versus fuel ratio for either fuel present before the fire, or fuel consumed during the fire. The Ward et al model is a function of the fuel ratio of the fuel present, the linear MCE model derived here a function of the fuel ratio of the fuel consumed. The fuel ratio is defined as the amount of grass fuel (live grass and grass litter) divided by total fuel amount (non-grass debris).

ACPD
12, 4243–4278, 2012

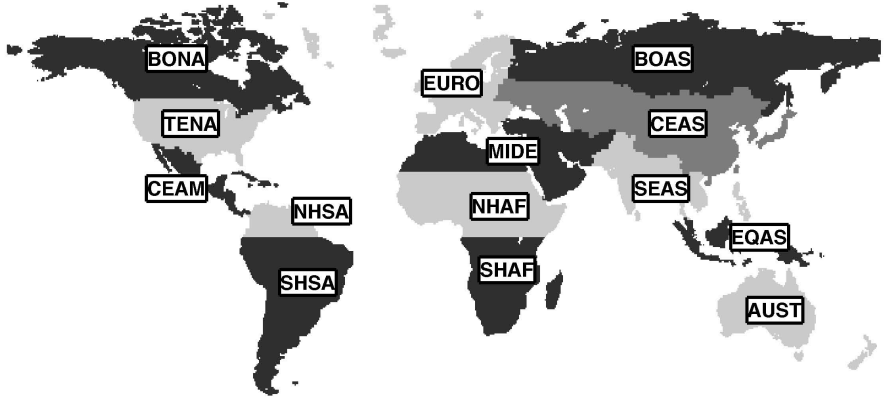

BONA	Boreal North America	NHAF	Northern Hemisphere Africa
TENA	Temperate North America	SHAF	Southern Hemisphere Africa
CEAM	Central America	BOAS	Boreal Asia
NHSA	Northern Hemisphere South America	CEAS	Central Asia
SHSA	Southern Hemisphere South America	SEAS	Southeast Asia
EURO	Europe	EQAS	Equatorial Asia
MIDE	Middle East	AUST	Australia and New Zealand

Fig. B1. GFED regions as used in this study (from Giglio et al., 2010).

ACPD
12, 4243–4278, 2012